Available on CMS information server

CMS NOTE 2003/011

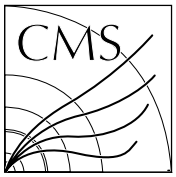

The Compact Muon Solenoid Experiment

CMS Note

Mailing address: CMS CERN, CH-1211 GENEVA 23, Switzerland

Feb 21, 2003

Simulation of the HPMT/VPT Light Collection Ratio

D. Britton, M. Apollonio[1], E. McLeod

Imperial College, London, England

Abstract

The ray tracing Monte Carlo, RAGE, is used to determine the amount of light expected to be collected by 20mm VPTs as used in the 1999 test-beam configuration, compared to the amount collected by HPMTs used in Lab-27 to view unwrapped crystals. This ratio will be used elsewhere to determine the performance of the VPTs and electronics chain during the test beam run. The ray-tracing simulations demonstrate the importance of the beveled crystal edges and show that the illumination of the rear-face of the crystal is uniform. However, it is shown that the amount of light collected does not scale simply with the detector size.

[1]Now at University of Trieste and INFN, Trieste, Italy

1 Introduction

In order to fully understand the performance of the VPTs and the electronics chain used in the 1999 test-beam, we wish to determine what fraction of the light was collected by the 20 mm active diameter VPT. Rather than estimating the absolute number, the ratio of light collected in the test beam configuration compared to that collected on the bench in Lab27 is simulated. In Lab27, an HPMT that covered the entire rear-face of the crystal was used to view unwrapped crystals. In the test-beam, the Lanthanum doped crystals were placed unwrapped in the carbon-fibre alveolar but had a reflective Tyvek end-piece at their tapered end. The Imperial College ray-tracing Monte Carlo, RAGE, is used to determine the ratio of light collected in these two geometries. The end-cap crystals had considerably better optical properties than previously, so the optical parameters in the simulation were updated.

2 Simulation Parameters

2.1 Geometry

The input cards to the simulation are contained in Appendix-1. The simulation consisted of a full size tapered end-cap crystal coupled to a circular photo-detector with optical grease. The beveled edges of the crystal have been included in the simulations for the first time and found to have a significant effect, as discussed below. The crystal was contained in an air-box, the reflectivity of which could be varied to simulate the crystal wrapping. For the test-beam set-up, the reflectivity of the box was assumed to by 5% to simulate the black alveolar, except at the tapered end where a 95% diffuse reflector was specified to simulate the Tyvek insert. The test-beam photo-detector had a 10 mm active radius and the reflectivity of the remainder of the rear face was set at 45% to approximate the aluminium insert. To simulate the Lab27 measurements, the reflectivity of the air-box was set to zero and the photo-detector radius set to 21.5mm, which covers the entire rear face of the crystal.

2.2 Refractive Index and Attenuation Length

An effective refractive index for Lead Tungstate was obtained by averaging the ordinary and extraordinary refractive indices from the measurements contained in Table-2 of CMS TN96-080. From these values, the Fresnel Transmission Limit for light passing longitudinally through a 220 mm long end-cap crystal was calculated using the expression:

$$F = \frac{(1-r)^2}{1-r^2} \qquad [1]$$

where r, the fraction of light reflected from an air-crystal boundary at normal incidence, is given in terms of the wavelength dependent refractive index n, by:

$$r = \left(\frac{1-n}{1+n}\right)^2. \qquad [2]$$

Equation-1 is the theoretical limit for transmission in the absence of any absorption within the crystal. The denominator is a series limit that accounts for the multiple reflections within the crystal. For a crystal of length L, the absorption coefficient (the reciprocal of the attenuation length) is then calculated from a comparison of the measured transmission T with the theoretical transmission limit F according to:

$$\mu = \frac{1}{L} \ln\left(\frac{F}{T}\right). \qquad [3]$$

The longitudinal transmission of the end-cap crystal 2193 measured at CERN was used to calculate the absorption coefficients for the simulation. The transmission was measured at 5nm intervals but specified in the simulation at 15nm intervals. For wavelengths (λ) of 420nm and above, the transmission is fairly constant and the three appropriate data points (λ–5, λ, λ+5 nm) were averaged to reduce the statistical fluctuations. Below 420nm, where the transmission changes rapidly, the measured values were used directly. Table-1 shows the data used and Figure-1 shows the calculated attenuation length as a function of wavelength.

Wavelength	*Refractive*	*Reflectivity*	*Fresnel Limit*	*Transmission*	*Abs. Coeff.*	*Attn. Length*
[nm]	*Index n*	*r*	*F*	*Data (2193)*	*μ [/mm]*	*[m]*
300	2.95	0.244	60.8%	0.4%	0.02300	0.04
315	2.69	0.210	65.3%	0.3%	0.02436	0.04
330	2.56	0.192	67.8%	0.3%	0.02450	0.04
345	2.47	0.180	69.5%	19.3%	0.00583	0.17
360	2.42	0.172	70.7%	52.0%	0.00139	0.72
375	2.37	0.166	71.5%	59.8%	0.00081	1.23
390	2.34	0.161	72.2%	64.7%	0.00050	2.01
405	2.32	0.158	72.7%	66.4%	0.00042	2.40
420	2.30	0.155	73.1%	67.3%	0.00038	2.62
435	2.28	0.153	73.5%	68.5%	0.00032	3.15
450	2.27	0.151	73.8%	69.5%	0.00027	3.68
465	2.26	0.149	74.0%	70.2%	0.00024	4.10
480	2.25	0.148	74.2%	70.4%	0.00024	4.13
495	2.24	0.147	74.4%	71.2%	0.00020	5.03
510	2.23	0.146	74.6%	72.0%	0.00016	6.37
525	2.23	0.145	74.7%	72.6%	0.00013	7.56
540	2.22	0.144	74.8%	73.0%	0.00011	9.07
555	2.22	0.143	75.0%	73.2%	0.00011	9.23
570	2.21	0.143	75.0%	73.5%	0.00010	10.25
585	2.21	0.142	75.1%	73.7%	0.00008	11.79
600	2.21	0.141	75.2%	74.0%	0.00007	13.48

Table-1: The Refractive Index and Transmission data used to determine the simulation parameters.

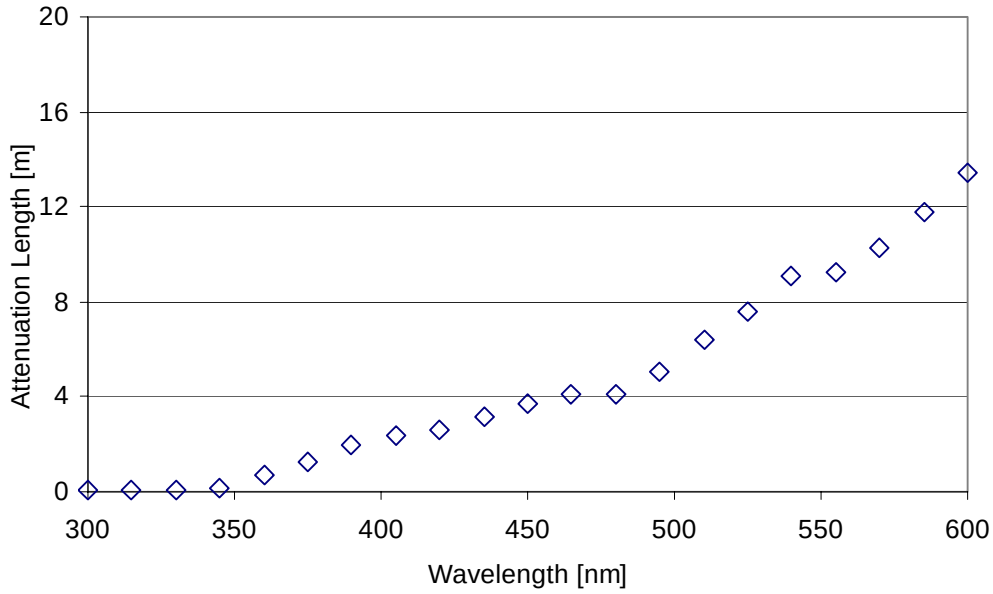

Figure-1: The calculated attenuation length as a function of wavelength.

2.3 Emission Spectrum and Detector Efficiency

The simulation requires as input the product of the emission spectrum and the photo-detector efficiency. The emission spectrum was taken from Page-31 of the ECAL TDR for Lanthanum doped crystals. The VPT and HPMT quantum efficiencies were taken from data from the respective manufacturers. The product of the emission spectrum and Quantum Efficiency gives the spectrum of the detected light. However, since these data are used in the simulation to define a set of equal probability bins (the integral of which is unity), the difference in the absolute quantum efficiency of the two devices is NOT included in the final ratio calculated.

Wavelength	*Emission*	*Quantum Effiencies*		*Emission x QE*	
	Spectrum	*H-VPT*	*HPMT*	*H-VPT*	*HPMT*
[nm]	*[relative]*	*[absolute]*	*[absolute]*		
300	0.000	0.21	0.27	0.0000	0.0000
325	0.012	0.21	0.26	0.0026	0.0031
350	0.148	0.22	0.25	0.0324	0.0369
375	0.457	0.21	0.25	0.0978	0.1120
400	0.790	0.21	0.25	0.1667	0.1967
425	1.000	0.20	0.23	0.2030	0.2270
450	0.807	0.20	0.20	0.1614	0.1630
475	0.556	0.17	0.18	0.0962	0.0973
500	0.391	0.15	0.15	0.0579	0.0594
525	0.247	0.11	0.13	0.0267	0.0321
550	0.132	0.07	0.11	0.0094	0.0145
575	0.078	0.04	0.09	0.0034	0.0070
600	0.062	0.01	0.06	0.0006	0.0037

Table-2: The emission spectrum of La-doped crystals and the quantum efficiencies of a Hamamatsu Vacuum Phototriode (H-VPT) and DEP Hybrid Photomultiplier (HPMT).

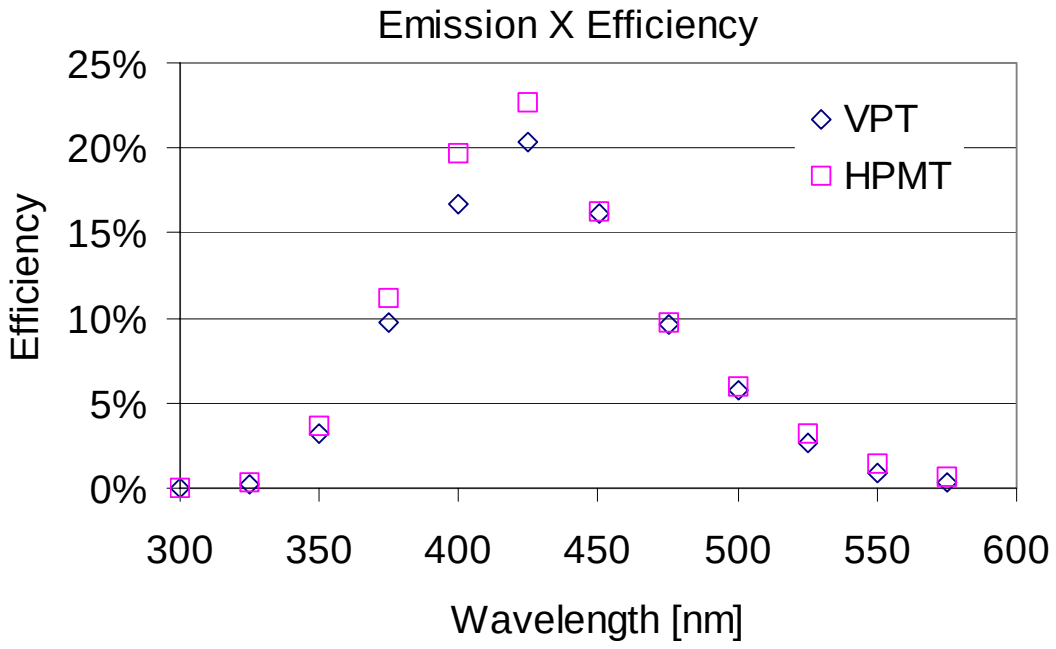

Figure-2: The product of the emission spectrum of La-doped crystals (TDR) and the photo-detector efficiency as a function of wavelength.

2.4 The Scatter Parameter and Crystal Bevels

Previous simulations contain a parameter that defined a characteristic re-scattering length for the photons necessary to reproduce the following data [*G.Davies, private communication*] from measurements made on end-cap crystals in Lab27 at CERN using the HPMT in early 1999:

1. Ratio of light yield of Mylar-wrapped crystals (5-sides) to naked crystals = 1.39 (average of three end-cap crystals).
2. Ratio of light yield of crystals with a Tyvek piece on the tapered end, to naked crystals = 1.21.
3. Ratio of light yield of crystals wrapped with Mylar on the four long sides and a Tyvek end-piece, to naked crystals = 1.45 (average of two end-cap crystals).

For this current work the geometrical description of the crystals was extended to include the non-polished bevels that join all six faces. These bevels are specified on the end-cap crystal drawing (1-TB-0054-100-00-A) to be between 0.5 and 0.7 mm (as shown in Figure-3). It was found that to reproduce the ratios given above, the bevel had to be set at the lower limit (0.5mm) and the scatter parameter set to zero. In other words, the scatter parameter appears to have previously accounted for the effect of the bevels and is no longer necessary. Examination of several crystals under a microscope found that the bevels varied considerably (even up the length of a crystal) but that 0.5 mm was not an untypical value. The sensitivity of the final result to the bevel size will be presented later.

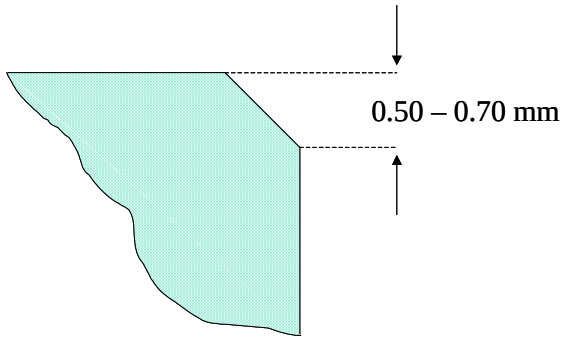

Figure-3: Engineering specification of the crystal edge bevels.

3 Ratio of Light Yields from Lab27 HPMT and Test-Beam VPT set-ups

The ratio of light collected by an HPMT covering the full rear-face of a completely naked crystal and a VPT with 20 mm active diameter viewing a crystal in the test-beam set-up (5% reflective alveolar, 45% reflective aluminium back-stop, and 95% reflective Tyvek front piece) is found to be 1.570 with a statistical error of 0.004. In the simulations the photons were produced isotropically with uniform weight over almost the entire width (±12mm from the centre line) of the crystal, at a position 65 mm from the front face. Systematic effects on this result are investigated in the following sections.

3.1 Sensitivity to Starting Depth

The light yields from Lab27 correspond to a source positioned 65 mm from the front face of the crystal. In the test beam, the data corresponds to showers that develop over the length of the crystal typically peaking at 70 mm from the front face. In the simulations the photons were started at a point 65 mm from the front face. Figure-4 shows that there is no significant variation of the final ratio as a function of starting position, except very close to the photo-detector.

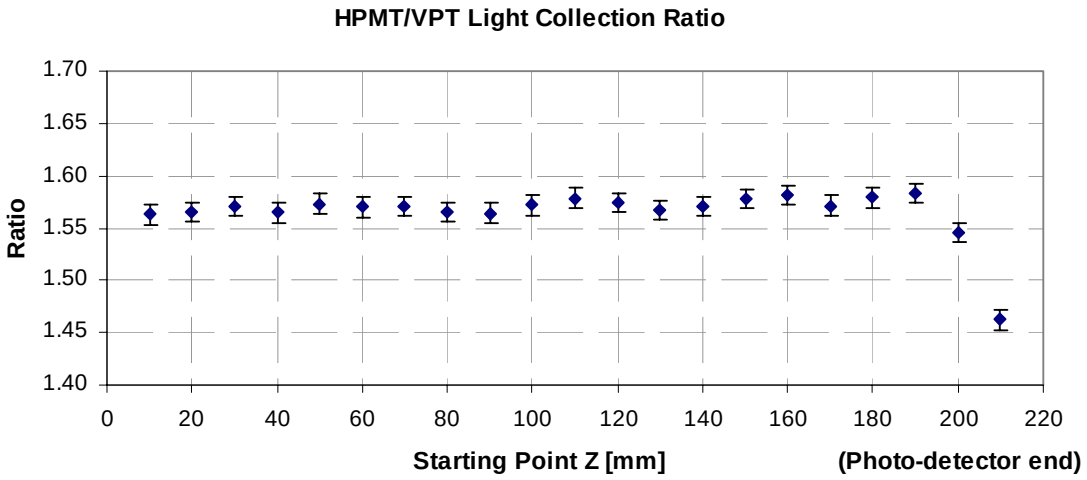

Figure-4: The ratio of light collected by the Lab27 HPMT to the test-beam VPT as a function of the light starting position.

3.2 Sensitivity to Stop Reflectivity

In the test-beam set-up the VPT did not cover the entire rear face of the crystal. The active area was modelled as a 20 mm diameter circle and the remaining area of the rear-face was assigned a reflectivity of 45% to simulate the (completely unknown) reflectivity of the aluminium insert in which the VPT was mounted. In practice, the geometry would have been somewhat more complicated with an annulus of glass around the active area and with an unknown space between the crystal and the insert that may or may not have contained optical grease. Figure-5 shows the effect on the ratio of varying the reflectivity of the aluminium insert in the simulation. The result is quite sensitive to this parameter and until some better estimate of the reflectivity can be made a large range should be considered: a value of ±0.08 on the ratio might be appropriate choice for a 1-σ error, corresponding to a reflectivity range of about 15% - 70%.

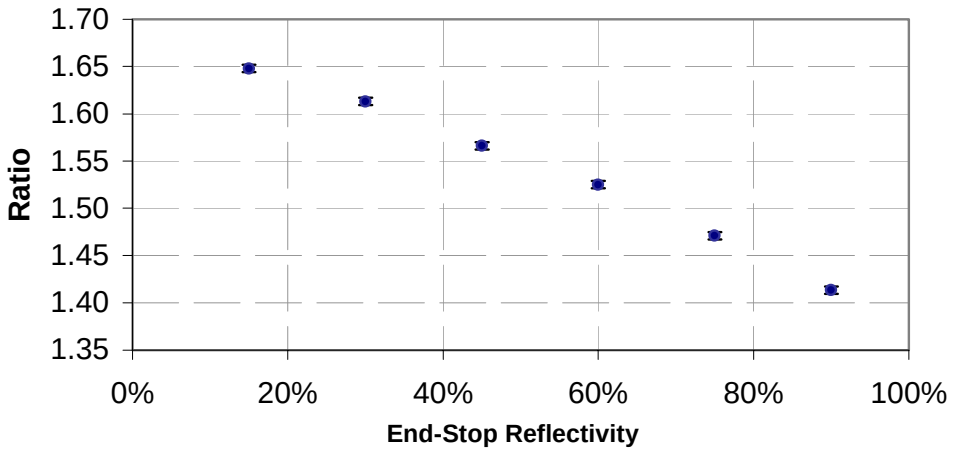

Figure-5: The ratio of light collected by the Lab27 HPMT to the test-beam VPT as a function of the reflectivity of the aluminium insert around the VPT.

3.3 Sensitivity to Alveolar Reflectivity

In the test-beam set-up, the crystal is supported in a black carbon-fibre alveolar that, in the simulations, was assumed to be 5% reflective. Figure-5 shows that varying this reflectivity over the range 0% - 30% has relatively little effect on the final ratio.

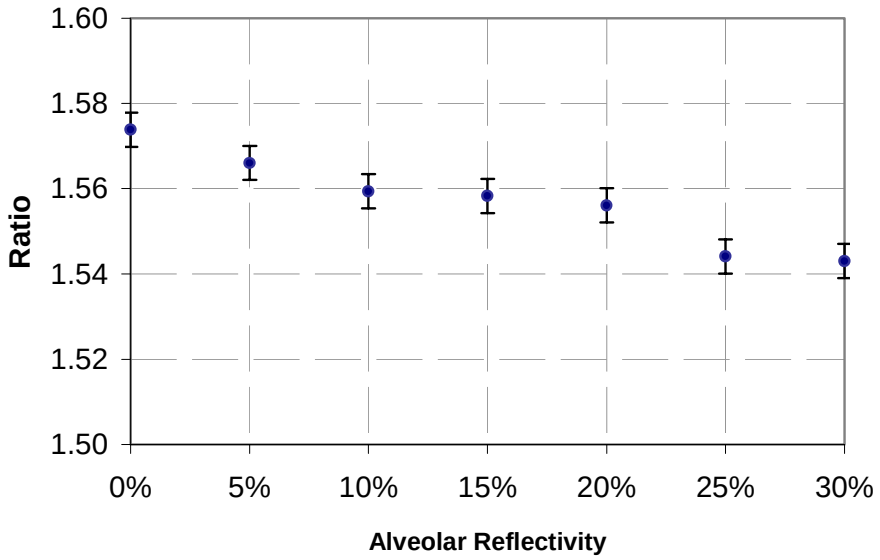

Figure-6: The ratio of light collected by the Lab27 HPMT to the test-beam VPT as a function of the reflectivity of the test-beam alveolar.

3.4 Sensitivity to Size of Bevels

The sensitivity of the final result to the size of the bevels is shown in Figure-6. Considering the uncertainty on (or variability of) the bevel dimension as +/- 0.2 mm, the error contribution to the final ratio is about 0.05.

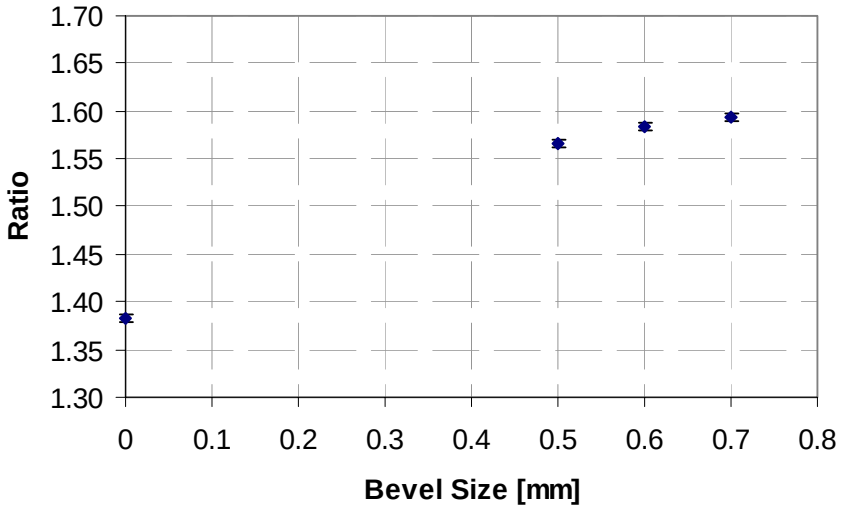

Figure-7: The ratio of light collected by the Lab27 HPMT to the test-beam VPT as a function of the bevel size.

3.5 Sensitivity to Refractive Index and Attenuation Coefficient

To test the stability of the result, the refractive index at all wavelengths was reduced by 0.1, which is approximately the difference between the ordinary and extraordinary refractive indices. The attenuation coefficient was recalculated from the transmission data of crystal 2193 and the simulations were repeated. The value of the ratio increased from 1.57 to 1.65. A 1-σ uncertainty of ± 0.08 on the ratio might therefore be appropriate.

3.6 Sensitivity to Emission Spectrum and Quantum Efficiency

The simulation uses the product of the emission spectrum and quantum efficiency, which appears as a set of equal probability bins in the NAITAB table (see Appendix-1). The emission spectrum obtained from the TDR was systematically shifted by about 12nm towards lower wavelengths to test the stability of the result. This simulation gave a value for the ratio of 1.59, compared to the baseline of 1.57. Swapping the quantum efficiencies of the VPT and HPMT, which are slightly different in both shape and magnitude (see Table-2), increased the ratio by 0.01. A total 1-σ uncertainty of ± 0.03 on the ratio might therefore be appropriate for these effects.

4 Final Result

The final result was obtained from a simulation where a large number of photons were traced, resulting in a negligible statistical error. The effective active area of the VPT photocathode is not known precisely. Reducing the active diameter from 20 mm to 19 mm changes the ratio from 1.57 to 1.68. The systematic error is estimated from combining this contribution (0.11) in quadrature with the contributions detailed above from the stop-reflectivity (0.08), the bevel size (0.05), the refractive index and attenuation length (0.08), and the emission spectrum and quantum efficiency (0.03). The final value for the ratio is 1.57 ± 0.17.

5 Understanding the Result

There are four factors that determine the ratio of light collected in the two cases: the different quantum efficiency of the photo-detectors, the different crystal wrappings, the different geometrical size of the detectors, and any non-uniformity of the light intensity on the rear-face of the crystal. These effects are investigated in the following sections.

5.1 Effect of Quantum Efficiency

A simulation was performed where the HPMT was given the same quantum efficiency as the VPT but there was no statistically significant change in the ratio of light collected. As noted earlier, the ratio calculated does not include the difference in the absolute value of the quantum efficiency (it only includes the different wavelength dependence of the quantum efficiencies). To make the final comparison between the HPMT and VPT configurations the calculated ratio must be scaled by the appropriate ratio of quantum efficiencies.

5.2 Effect of Wrapping

The simulation of the test-beam set-up was re-run with the HPMT in place of the VPT. Comparison with the LAB27 simulations showed a 15.7% increase in light collection that can be attributed to the Tyvek end-piece that was present in the test-beam but not in the Lab27 measurements. The influence of the end-piece increases as the photo-detector size decreases. For example, simulating the VPT on the Lab27 set-up showed a 26% decrease in light as compared to the test-beam set-up with VPT.

5.3 Effect of Geometrical Size

The solid curve in Figure-7 shows the geometrical acceptance of a circular detector centred on the rear face of an end-cap crystal. The points are the results of simulations of the test-beam set-up where the radius of the photo-detector has been varied (normalised to 100% for a photo-detector that covers the entire rear face). It can be seen that the actual fraction of light collected by a 10mm active diameter VPT is 53.8%, compared with the 34.9% expected from purely geometrical considerations.

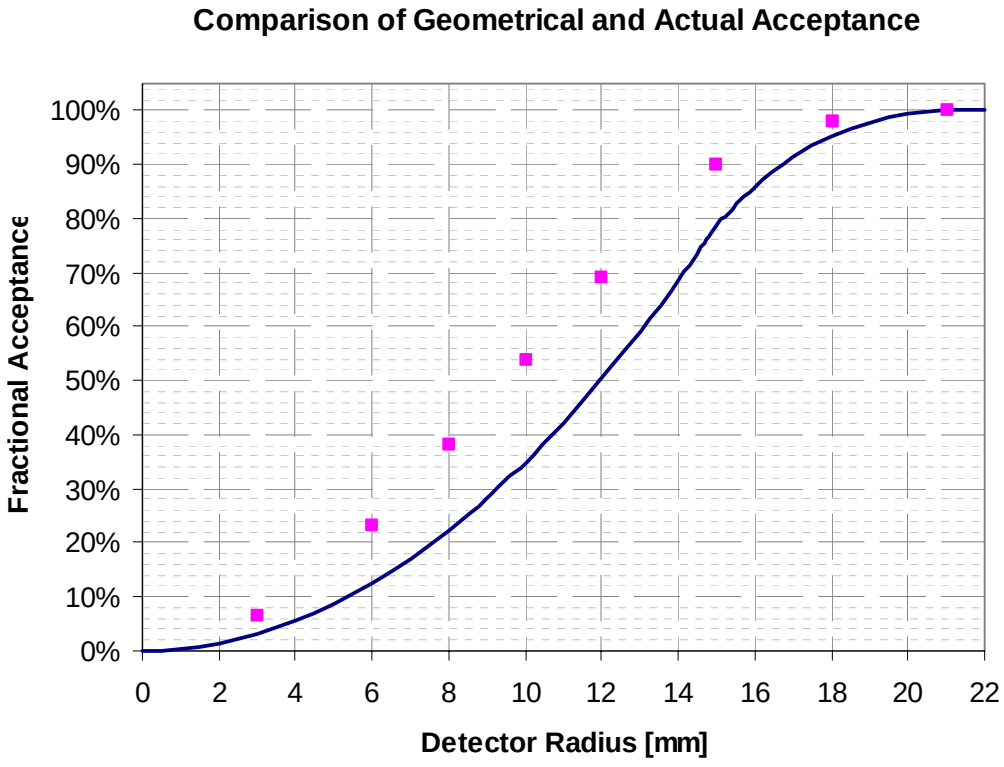

Figure-8: Geometrical acceptance (solid curve) compared with simulation results (points).

5.4 Illumination Uniformity

The fact that the amount of light collected by the VPT is greater than expected from geometrical considerations suggests that the illumination of the rear-face of the crystal is not uniform. However, this is not the explanation: Figure-8 shows a density plot of detected photons on the plane of the photo-detector and there is no peaking towards the centre. The reason that the amount of detected light is larger than the geometrical expectation lies in the fact that photons that miss the VPT are reflected around the crystal and have many subsequent chances of detection. To be consistent with a uniform distribution, this probability must be about 29%. This effect arises partly from the reflectivity of the aluminium backstop and partly because the crystal-air boundary around the VPT internally reflects more than the boundary between the crystal and optical-grease. To verify this, a simulation was performed with a 20mm VPT surrounded by black material with the optical grease covering the entire rear-face. The value expected from purely geometrical considerations was then obtained.

6 Conclusion

The final value obtained for the ratio of light collected by the HPMT in Lab27 to the VPT in the test-beam is estimated to be 1.57 ± 0.17. This ratio may be understood to arise from a 15.7% loss due to the missing Tyvek reflector at the front of the crystal in Lab27, combined with a geometrical acceptance factor of 34.9% for the VPT compared to the HPMT, and to the fact that the remaining 65.1% of the light has a 29% chance of being subsequently detected after multiple reflections. That is, the ratio is given by: $0.843/(0.349 + 0.651 * 0.29) = 1.57$.

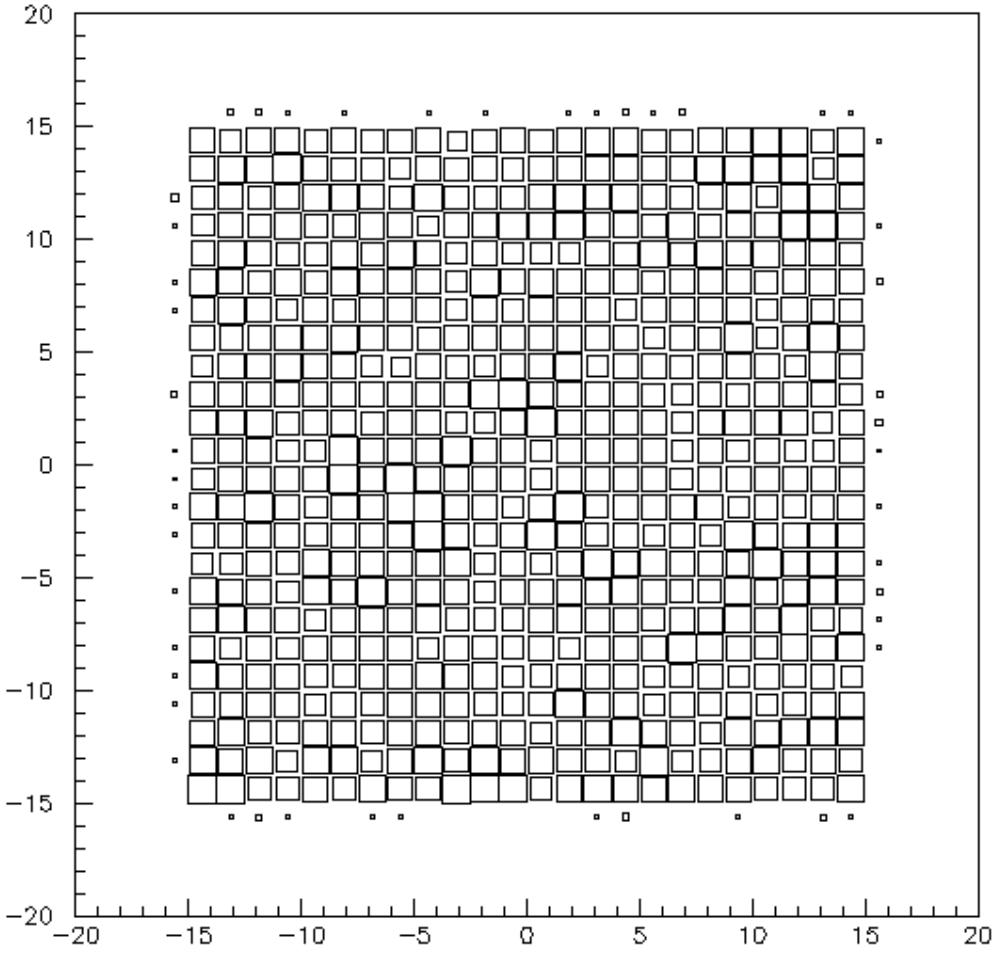

Figure-9: Uniformity of illumination across the photo-detector: a box plot of the density of detected photon hits. *The scales are in millimeters.*

Appendix: Sample input cards to the RAGE simulations

```
/*
Testbeam geometry: 20mm diameter VPT
*/

batch
caquik 0 /* switch photo-cathode simulation at start */
ntub 1 1 /* Single tube (notional detector) */

/* Integrated emission spectrum X Efficiency of VPT detector. */
NAITAB 20  300.000 360.112 376.203 384.734 393.266 401.286
           407.390 413.494 419.597 425.711 431.904 438.097
           444.289 450.681 459.441 468.201 478.279 492.922
           513.782 600.000

SPOT -12.0
SCATTER 1 0.
SCATTER 2 0.
SCATTER 3 0.
SCATTER 4 0.

geom
/* Objects.  Name            <-- X,Y,Z -->  < Angles >  Obj Shp Mat */
object 1 'Crystal'           0.  0.    0.0   0.  0.  0.   4   1   1
object 2 'Optical Gel 1'     0.  0.  220.025 0.  0.  0.   4   2   2
object 3 'Detector'          0.  0.  220.055 0.  0.  0.   4   3   3
object 4 'Air box 1'         0.  0.    0.0   0.  0.  0.   0   4   4

/* Materials. Name   Ref Att */
material 1 'PbWO4'    1   1
material 2 'Grease'   2   2
material 3 'Quartz'   3   0
material 4 'Air'      4   0

/* Refractive index tables.
       # Nbn Low  Hig    Values....   */
refind 1 20  300  585    2.950 2.694 2.558 2.474 2.416
                         2.375 2.344 2.319 2.300 2.284
                         2.270 2.259 2.250 2.241 2.234
                         2.228 2.222 2.217 2.213 2.209
refind 2 0               1.7
refind 3 0               1.46
refind 4 0               1.0

/* Attenuation tables.
      # Nbn Low  Hig    Values....   */
atten 1 20  300  585 0.02300 0.02436 0.02450 0.00583 0.00139
                     0.00081 0.00050 0.00042 0.00038 0.00032
                     0.00027 0.00024 0.00024 0.00020 0.00016
                     0.00013 0.00011 0.00011 0.00010 0.00008
atten 2  0           0.000010

/* ---------------   define the shapes.   -------------- */

begin shape 1 4 0 /* scintillator */
vertex   1    14.5 -15.0    0.5
```

```
vertex    2    -13.1     -15.0     0.5
vertex    3    -13.6     -14.5     0.5
vertex    4    -13.6     13.1 0.5
vertex    5    -13.1     13.6 0.5
vertex    6    14.5 13.6 0.5
vertex    7    15.0 13.1 0.5
vertex    8    15.0 -14.5     0.5
vertex    9    14.5 -15.0     219.5
vertex    10   -14.5     -15.0     219.5
vertex    11   -15.0     -14.5     219.5
vertex    12   -15.0     14.5 219.5
vertex    13   -14.5     15.0 219.5
vertex    14   14.5 15.0 219.5
vertex    15   15.0 14.5 219.5
vertex    16   15.0 -14.5     219.5
vertex    17   14.5 -14.5     0.0
vertex    18   -13.1     -14.5     0.0
vertex    19   -13.1     13.1 0.0
vertex    20   14.5 13.1 0.0
vertex    21   14.5 -14.5     220.0
vertex    22   -14.5     -14.5     220.0
vertex    23   -14.5     14.5 220.0
vertex    24   14.5 14.5 220.0

face 1 3 4   7 15 16 8
face 2 3 4   5 13 14 6
face 3 3 4   3 11 12 4
face 4 3 4   1 9 10 2
face 5 3 4   24 23 22 21
face 6 3 4   17 18 19 20
face 7 3 4   10 11 3 2
face 8 3 4   16 9 1 8
face 9 3 4   14 15 7 6
face 10 3 4  12 13 5 4
face 11 3 4  3 4 19 18
face 12 3 3  2 3 18
face 13 3 4  18 17 1 2
face 14 3 3  17 8 1
face 15 3 4  17 20 7 8
face 16 3 3  20 6 7
face 17 3 4  20 19 5 6
face 18 3 3  19 4 5
face 19 3 3  23 13 12
face 20 3 4  23 12 11 22
face 21 3 3  22 11 10
face 22 3 4  22 10 9 21
face 23 3 3  21 9 16
face 24 3 4  21 16 15 24
face 25 3 3  24 15 14
face 26 3 4  24 14 13 23
end shape

begin shape 2 1 0 cylinder 1 10.0 0.05 end shape   /* Grease */
begin shape 3 1 1 cylinder 2 10.0 0.01 end shape   /* VPT det. */

begin shape 4 4 0  /* air box 1 */
vertex 1  15.02  -15.02 -0.02
vertex 2 -13.62  -15.02 -0.02
vertex 3 -13.62   13.62 -0.02
vertex 4  15.02   13.62 -0.02
```

```
vertex 5  15.02  -15.02 220.07
vertex 6 -15.02  -15.02 220.07
vertex 7 -15.02   15.02 220.07
vertex 8  15.02   15.02 220.07
face 1 3 4   1 4 8 5
face 2 3 4   3 7 8 4
face 3 3 4   2 6 7 3
face 4 3 4   1 5 6 2
face 5 3 4   8 7 6 5
face 6 3 4   1 2 3 4
end shape


/* -------Boundaries. N.B. Define each boundary once only !! ------- */
/*       Shp1 Fac1 Shp2 Fac2 Type  Reflec.  Grind  Lambert */
boundary   1   1    4    0    1      0.0     0.0     0  /*Scint. +X side */
boundary   1   2    4    0    1      0.0     0.0     0  /*Scint. +Y side */
boundary   1   3    4    0    1      0.0     0.0     0  /*Scint. -X side */
boundary   1   4    4    0    1      0.0     0.0     0  /*Scint. -Y side */
boundary   1   5    2    2    1      0.0     0.0     0  /*Scint. - Gel 1 */
boundary   1   5    4    0    1      0.0     0.0     0  /*scint. - airgap*/
boundary   1   6    4    0    1      0.0     0.0     0  /*Scint. -Z side */
boundary   1   7    4    0    1      0.0     0.2     0  /*all the bevels */
boundary   1   8    4    0    1      0.0     0.2     0
boundary   1   9    4    0    1      0.0     0.2     0
boundary   1  10    4    0    1      0.0     0.2     0
boundary   1  11    4    0    1      0.0     0.2     0
boundary   1  12    4    0    1      0.0     0.2     0
boundary   1  13    4    0    1      0.0     0.2     0
boundary   1  14    4    0    1      0.0     0.2     0
boundary   1  15    4    0    1      0.0     0.2     0
boundary   1  16    4    0    1      0.0     0.2     0
boundary   1  17    4    0    1      0.0     0.2     0
boundary   1  18    4    0    1      0.0     0.2     0
boundary   1  19    4    0    1      0.0     0.2     0
boundary   1  20    4    0    1      0.0     0.2     0
boundary   1  21    4    0    1      0.0     0.2     0
boundary   1  22    4    0    1      0.0     0.2     0
boundary   1  23    4    0    1      0.0     0.2     0
boundary   1  24    4    0    1      0.0     0.2     0
boundary   1  25    4    0    1      0.0     0.2     0
boundary   1  26    4    0    1      0.0     0.2     0

boundary   2   1    3    2    1      0.0     0.0     0  /*Gel 1 - quartz */
boundary   2   3    4    0    1      0.0     0.0     0  /*Gel 1 - airgap */

boundary   3   1    0    0    4      0.0     0.0     0  /*detector target*/
boundary   3   3    0    0    1      0.0     0.0     0  /*quartz side */
boundary   4   1    0    0    2      0.05    0.00    0  /* Air 1 +X side */
boundary   4   2    0    0    2      0.05    0.00    0  /* Air 1 +Y side */
boundary   4   3    0    0    2      0.05    0.00    0  /* Air 1 -X side */
boundary   4   4    0    0    2      0.05    0.00    0  /* Air 1 -Y side */
boundary   4   5    0    0    2      0.45    0.00    0  /* Air 1 +Z side */
boundary   4   6    0    0    2      0.95    0.00    1  /* Air 1 -Z side */

return
```